

# Physical property characterization of $\text{Cu}_{x(1,2)}\text{O}$ nanofilms grown on (100) silicon by thermal copper oxidation

Joel Díaz-Reyes, José Eladio Flores-Mena, Roberto Saúl Castillo-Ojeda, José M. Gutiérrez-Arias, and María Montserrat Morín-Castillo

**Abstract**—Cuprous oxide ( $\text{Cu}_2\text{O}$ ) and cupric oxide ( $\text{CuO}$ ) films of nanometric thicknesses on monocrystalline (100) silicon were grown by thermal copper oxidation technique. The copper nanofilms were deposited on crystalline (100) silicon by autocatalysis using watery solutions based on copper sulphate ( $\text{CuSO}_4$ ) and hydrofluoric acid (HF). The  $\text{Cu}_2\text{O}$  was obtained at an annealing temperature of  $200^\circ\text{C}$ , whereas for the  $\text{CuO}$  was necessary to use a higher oxidation temperature,  $600^\circ\text{C}$  for 3 h. The thicknesses of the copper oxide layers were ranged from 30 to 150 nm obtained by ellipsometry. For the characterization of the oxidized copper layers, cuprous and cupric of oxides, were used different techniques. In order to examine the surface morphology of the films atomic force microscopy (AFM) was used and for the identification of the different oxides crystalline phases was used X-ray diffraction. By means of the Debye-Scherrer equation the nanocrystal size that forms the copper-based nanofilms was estimated. For the Cu nanofilm in the diffraction peak (111), a crystal size of 16.82 nm is obtained. Similarly, for  $\text{Cu}_2\text{O}$ , the nanocrystal size is 8.11 nm and for the  $\text{CuO}$ , the size is 6.66 nm, which indicates that crystal size depends of the annealing temperature. The refractive indexes measured for the nanofilms oxidized at  $200^\circ\text{C}$  was from 2.2-2.3 and for the obtained ones at  $600^\circ\text{C}$  was from 2.7-2.9.

**Keywords**—AFM,  $\text{Cu}_x\text{O}$ , thermal oxidation technique, XRD.

## I. INTRODUCTION

THE interest by the study and preparation of copper oxide thin layers is by their use in the manufacture of toxic gas sensor elements [1,2]. The Cu–O system has two stable oxides: cupric oxide ( $\text{CuO}$ ) and cuprous oxide ( $\text{Cu}_2\text{O}$ ). These

J. Diaz-Reyes is with the Center for Research in Applied Biotechnology, Instituto Politécnico Nacional. Ex–Hacienda de San Molino. Km 1.5 de la Carretera Estatal Santa Inés Tecuexcomac-Tepetitla. Tepetitla, Tlaxcala. 90700. México (phone: +00 52 (55) 5729600 ext. 87828; e-mail: joel\_diaz\_reyes@hotmail.com).

J. E. Flores-Mena is with the Faculty of Sciences of the Electronics, Benemérita Universidad Autónoma de Puebla. Av. San Claudio y 18 Sur, Ciudad Universitaria, Puebla, Puebla. 72570. México.

R. S. Castillo-Ojeda is with the Universidad Politécnica de Pachuca (UPP). Carretera Pachuca Cd. Sahagún Km. 20, Rancho Luna, Ex-Hacienda de Santa Bárbara, Zempoala, Hidalgo. 43830. México.

J. M. Gutiérrez-Arias is with the Faculty of Sciences of the Electronics, Benemérita Universidad Autónoma de Puebla. Av. San Claudio y 18 Sur, Ciudad Universitaria, Puebla, Puebla. 72570. México.

M. M. Morín-Castillo is with the Faculty of Sciences of the Electronics, Benemérita Universidad Autónoma de Puebla. Av. San Claudio y 18 Sur, Ciudad Universitaria, Puebla, Puebla. 72570. México.

two oxides are semiconductors with band gaps in the visible or near infrared regions. These materials have several advantages: (i) availability and abundance of the starting materials, (ii) non-toxic nature, (iii) low production cost, (iv) band gaps lie in an acceptable range for solar energy conversion, and (v) n- and p-type conductivity [3,4]. As a result, copper oxides have found numerous applications in diverse fields such as solar cells and photovoltaic materials [4], electrochromic coatings [5], catalytic applications [6], and high-Tc superconductors [7]. Doped copper oxide thin films have found applications such as in the fabrication of p-type transparent conductors [8]. The Cu-O layers are also used in photoconductive devices as the photovoltaic cells and are important part of one of the families of superconducting at high temperatures [9]. The crystalline phases of copper oxide are the cupric oxide or tenorite ( $\text{CuO}$ ) and the cuprous oxide or cuprite ( $\text{Cu}_2\text{O}$ ). Both materials behave like p-type semiconductors, and the band gap energy  $\text{CuO}$  is of 1.51 eV and 2.0 eV for the  $\text{Cu}_2\text{O}$  at room temperature [10,11]. The refractive index of the  $\text{CuO}$  is of 2.21 and 2.741 for the  $\text{Cu}_2\text{O}$ , to the wavelength of 623.8 nm [11,12].

With object to obtain control over some of the copper oxide phases, various studies on the formation of layers of Cu-O have been reported in literature using different growth techniques. Some of them used to prepare copper oxide thin layers of a single phase are: chemical deposit in phase vapour [13,14], electrodeposition [15] and molecular beam epitaxy (MBE) [16]. Although, it is difficult to obtain thick layers of Cu-O of a single phase by the technique of thermal oxidation [17,18] is possible to obtain a single phase if the copper layer is sufficiently thin and with a predominant crystalline orientation as infers of the experiments of oxidation of copper monocrystals [19]. In contrast, the process of monocrystal oxidation of copper, where the process is controlled by diffusion, in the oxidation of nanometric layers the process is restricted to the surface and will be controlled by the type of adsorption sites [20]. For the case of deposited copper nanolayers, in their initial crystalline orientation influences the crystalline orientation of the substrate where they were deposited [21]. The type of adsorption sites changes according to the adjustments that atoms acquire from the surface with the temperature. For temperatures close to  $400^\circ\text{C}$  has identified

that the O-Cu-O structure has an energy of activation very small and it is related to the structure of the  $\text{Cu}_2\text{O}$  [22,23].

In this work, the obtaining of Cu-O nanolayers by the technique of thermal oxidation of nanometric copper layers is reported. The main objective was to obtain copper oxide layers of a single crystalline phase on monocrystalline silicon substrates. As it will be described more below CuO and  $\text{Cu}_2\text{O}$  layers with thicknesses of some tens of nanometres were obtained. The crystallographic characteristics of the copper layer, the oxidation atmosphere and the oxidation temperatures were determining for the obtaining of the wished crystalline phases.

## II. EXPERIMENTAL DETAILS

The copper nanolayers were deposited on monocrystalline (100) silicon substrates using an autocatalytic process [24]. The electrochemical bath is a watery copper sulphate solution ( $\text{CuSO}_4 \cdot 5\text{H}_2\text{O}$ ) 0.01 molar and hydrofluoric acid (HF) (49%), in a proportion of 100:1 in volume. As substrates were used (100) silicon wafers p-type with resistivity of 1-5  $\Omega\text{-cm}$  and  $15 \times 15 \text{ mm}^2$  of area. The preparation of the substrates surface consisted of two stages. The first one was a cleaning RCA type using the procedures described in the reference [25], and in second one, the silicon wafers were submerged in a watery solution of HF (49%) at 10% for passivating the silicon surface [26]. For the samples studied in this work, the copper layers were deposited by immersion of the substrates in the chemical bath by 30 and 90 s. The deposit times were selected of such a way that the thicknesses were not greater than 100 nm. In order to assess the influence of the HF concentration on the physical characteristics of the copper and Cu-O layers, it was prepared another group of samples with different HF concentrations in the solution as is indicated in Table 1. For the oxidation of these layers was not used special mixture of gases as atmosphere, the oxidation was performed in the laboratory air-atmosphere using 200 and 600°C as oxidation temperatures for 3 h. The degree of oxide conversion of the copper layers was determined measuring their refractive indexes as function of the oxidation time. Another group of samples with similar characteristics was used as a control group for a better comparison of the results obtained in the processes. This group of copper layers was subjected to similar processes in high purity nitrogen atmosphere. In this case, the Cu nanolayers did not show appreciable changes in their physical characteristics.

The thicknesses, refractive indexes of the copper layers and the crystalline phases of copper oxide were determined by ellipsometry measurements with an Ellipsometer Gaertner L117 model. The layers surface morphology was examined with an atomic force microscope (AFM) model CP0175 Autoprobe of Park Scientific Instruments. The structural characterization of the layers was carried out by X-ray diffraction in a system SIEMENS D5000.

**Table 1.** Experimental conditions for the deposit of copper layers on (100) silicon with different HF concentrations by thermal oxidation technique.

Sample	Time (s)	$\text{CuSO}_4$ (ml)	HF (ml)
Cu8	30	39.6	0.4
Cu10	30	39.2	0.8
Cu12	30	38.8	1.2
Cu14	39	38.4	1.6
Cu41	90	39.6	0.4
Cu42	90	39.2	0.8
Cu43	90	38.8	1.2
Cu44	90	38.4	1.06

## III. EXPERIMENTAL RESULTS AND DISCUSSION

Fig. 1 shows two typical topographical images acquired with the AFM of the surface morphology of the copper layers on (100) silicon. The samples showed in figure were deposited using times of a) 30 and b) 90 s, samples Cu8 and Cu41. As can be noticed, the copper layers are constituted of almost spherical appearance particles. In the obtained layers using solutions with the same molarity, the particle dimensions increase with the increase of the immersion time.

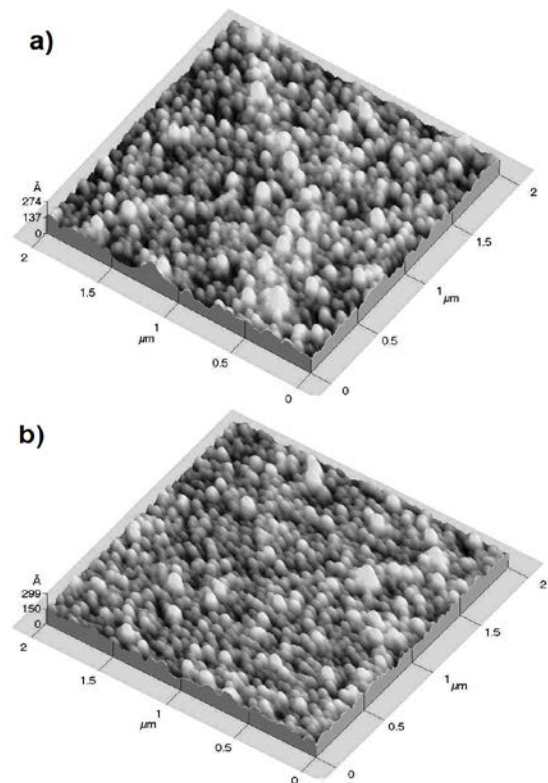


**Fig. 1.** Surface morphology of the typical copper layers on (100) silicon obtained by AFM with two immersion times: a) 30 and b) 90 s, samples Cu8 and Cu41.

For the deposition times used in this work, the copper particles did not completely cover the substrate surface. An estimation based on the AFM microphotographies indicates that the spherical nanoparticles have diameters ranging from 80 to 100 nm. The measured average roughness is of  $\sim 26.2 \text{ \AA}$  for nanolayers with 30 s of immersion, see Fig. 1a, and  $20 \text{ \AA}$

for those ones with 90 s of immersion, as can be appreciated in Fig. 1b; additionally the diminution in surface roughness can be related to the increase in the nanofilms density.

Fig. 2 shows the behaviour of the thickness as function of the HF concentration used for depositing the copper nanolayers, which was measured by ellipsometry. In this figure can be observed that the increase in the HF concentration is accompanied by a slight increase in the layers thickness. The dash lines in figure are included only to indicate the tendency observed in the total set of data that have been analysed. From this figure can be clearly noted that the copper layers thickness does not vary linearly with the immersion time. Unlike of the results obtained for the case of layers of several micrometres of thickness, where a parabolic dependency is observed with the immersion time as was observed by Lee et al. [24]. However, the small range of variation in the thicknesses of our layers did not allow a clear identification of the dependence of the layer thickness with the immersion time.

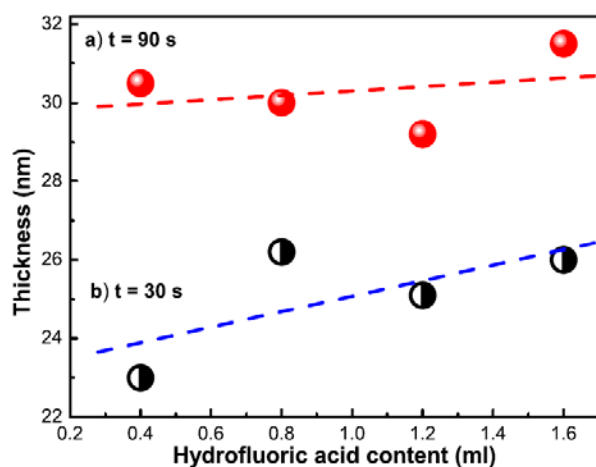


Fig. 2. Thickness of the deposited copper layers as function of the HF concentrations for two deposit times: a) 90 and b) 30 s.

It is perceptible of the XRD patterns obtained from the nanofilms in  $2\theta$  ranging  $30\text{--}60^\circ$  that these are polycrystalline, see Fig. 3. The X-rays diffraction patterns for each type of nanolayer were included in figure. Although, the peaks present in the diffractograms are weak as a consequence of the nanometric thickness of the layers. The diffraction peaks at  $43.43$  and  $50.57^\circ$  obtained from the as-deposited films associated to diffraction planes (111) and (200) were matched with the standard Cubic Cu phase (ICDD File: 04-0836; space group #225). The reflection from (111) plane was found to be the strongest orientation, which indicate that the particles have a preferential crystallographic orientation in the direction (111), with a small percentage in the direction (200). The peak at  $36.64^\circ$  possibly associated at (111) plane of cuprous oxide ( $\text{Cu}_2\text{O}$ ), which lead to the mixed Cu– $\text{Cu}_2\text{O}$  phase. The layers obtained with different HF concentrations in the solutions did not change appreciably in their X-ray diffractograms presented above. After the process of oxidation of the Cu samples by a minimum time of 60 min at  $200^\circ\text{C}$ , the surfaces presented noticeable changes that were visible at naked eye. A

diffraction peak from the (111) plane of cubic  $\text{Cu}_2\text{O}$  (ICDD File: 05-0667; space group #224) was obtained at  $36.53^\circ$ . A single  $\text{Cu}_2\text{O}$  phase was obtained for the films annealed at  $200^\circ\text{C}$ , with a strongest orientation along (111) plane. When the annealing temperature is increased to  $600^\circ\text{C}$ , the  $\text{Cu}_2\text{O}$  phase transforms into copper (II) oxide (cupric oxide; CuO) phase [5,7,14]. The diffraction peaks of (-111) and (200) from the monoclinic CuO phase were identified from the standard data (ICDD File: 45-0937 and 48-1548; space group #15). By means of the Debye-Scherrer equation, the nanocrystal size that forms the copper-based nanofilms can be estimated. For the as-deposited film, in the diffraction peak (111) a crystal size of 16.82 nm and a lattice constant ( $a$ ) of  $3.61 \text{ \AA}$  are obtained. Similarly for  $\text{Cu}_2\text{O}$ , the nanocrystal size is 8.11 nm and  $a = 4.26 \text{ \AA}$ . Finally, for the tenorite (CuO), the crystal size is 6.66 nm and  $a = 4.58 \text{ \AA}$ . The conversion of  $\text{Cu}_2\text{O}$  to CuO during heating in the presence of oxygen is well known [27]. These results indicate that as the thermal treatment temperature increases, the crystal size decreases. It is earlier reported by Nair et al. [28] that the  $\text{Cu}_2\text{O}$  phase convert into CuO phase when annealed at  $350^\circ\text{C}$ , which corroborate in the present work. The composition of CuO is maintained even for the annealing at  $450^\circ\text{C}$ . It is also reported that at still higher temperature, CuO could revert to  $\text{Cu}_2\text{O}$  [29], but this possibility of crystalline phase transformation was not found in the present work. For annealing temperatures smaller at  $200^\circ\text{C}$  the layers reached a tonality blue-intense and for higher annealing temperatures the layers were of grayish-blue colour. The refractive indexes measured for the layers oxidized at  $200^\circ\text{C}$  was from 2.2 to 2.3 and for the obtained ones at  $600^\circ\text{C}$  was from 2.7 to 2.9, which corroborate the change of crystalline phase due to the increase in annealing temperature.

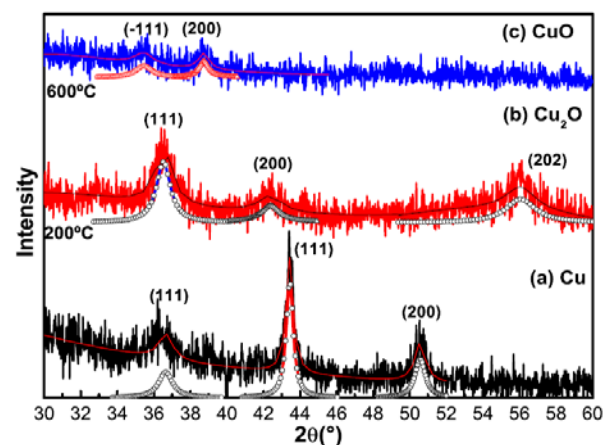


Fig. 3. X-rays diffraction spectra for the Cu and Cu-O layers.

The refractive index data and the X-ray diffraction information demonstrate that with the used experimental conditions used in the present work is possible to obtain copper oxide layers with a single phase in each case only by increasing the annealing temperature. The variation range indicated for the measured refractive index can be associated to the roughness degree of the nanolayers [7]. In Fig. 4 is

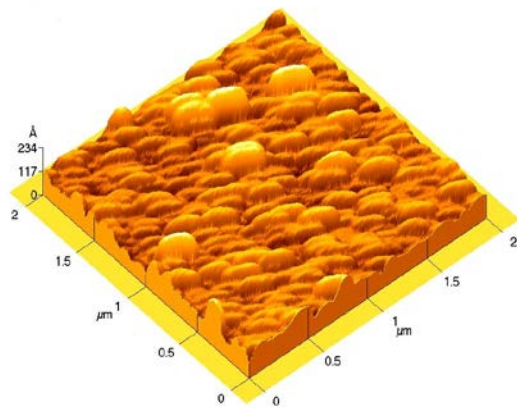


Fig. 4. Superficial morphology for the copper oxide layers by AFM.

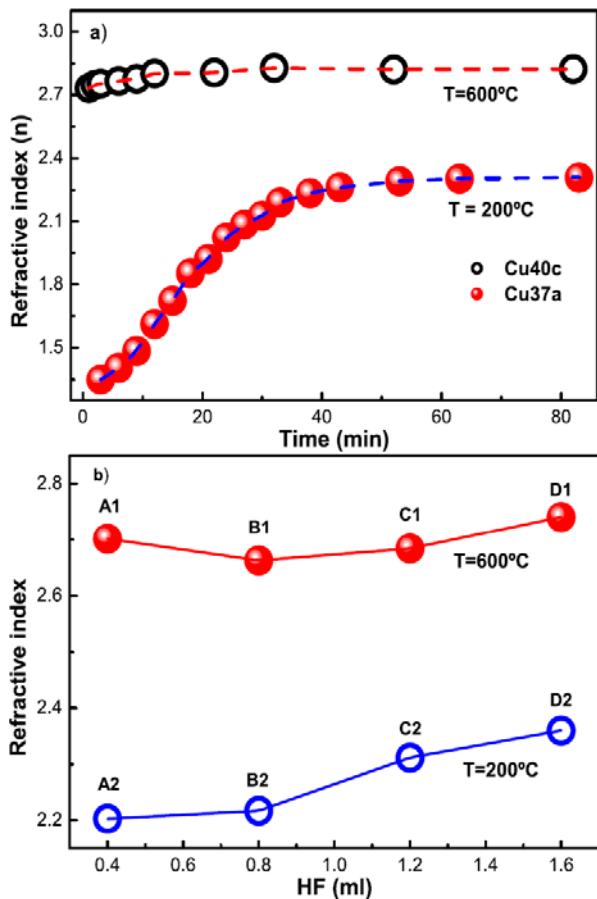


Fig. 5. Behaviour of the refractive index for copper oxide layers deposited by thermal oxidation: a) as function of the oxidation time for a HF concentration of 0.1 ml and b) as function of HF concentrations with an oxidation time of 60 min.

shown a typical AFM topography surface image of the copper oxide layers. The roughness of this layer is of 18.5 Å and is smaller than the initial roughness of the copper layers.

In order to study the behaviour of the refractive index of the copper layers, the samples refractive indexes were measured and plotted as function of the annealing temperature, HF concentration and used deposition time. As is shown in Fig. 5, from these measurements, it was observed that the copper

oxide layers, regardless the different oxidation times and for the two used temperatures present a defined crystalline phase after a minimum time of 40 min. The transformation to the cuprite crystalline phase takes place in a shorter time than the required for the transformation to tenorite crystalline phase. Similar results for copper layers were observed with thicknesses of up to 100 nm, which indicates that at least for the indicated thicknesses range the formation of the phases do not depend on the layers initial thickness.

According to the results of X-ray diffraction, after the oxidation processes the Cu-O layers have a well-defined orientation, so that, in the formation of the copper oxide crystalline phases influences the initial structural order of copper particles on the silicon substrate. The selected oxidation atmosphere and temperatures have also a crucial role for the formation of the crystalline phase. Since the copper layers are constituted by small crystal with preferential orientation in the direction (111), the oxidation of themselves takes place at different ratios according to the different faces from the small copper crystals.

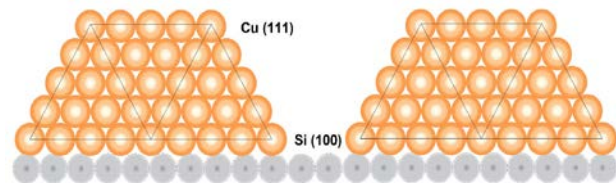


Fig. 6. Possible adjustment of the small copper crystals on the silicon surface with direction (100). The atoms are not to scale and the sizes only are illustrative.

Different studies [23,30] have shown than for oxidation temperatures close to 200°C, the copper oxidation rate diminishes according to the sequence in the crystalline planes (100), (111), (110) and (311), and that the oxidation rate in the surfaces with orientation (100) and (111) is at least twice greater than in the other directions. In addition, the oxidation rate in the planes (100) is at least three times greater than for the planes (111), this difference increases for oxidation temperatures higher than 200°C.

The difference increases until in a factor of 10 for the orientations (110) and (311), in such a way that the oxidation rate of the copper layers between the small crystals (in the parallel line of the substrate surface) is greater than the oxidation rate in the perpendicular direction (direction (111)). The difference in the oxidation rates for the different crystalline directions allows to explain the conservation in the degree of order of the layers, according to the X-ray diffraction results as the decreasing in the oxidized layers roughness with respect to the initial copper layers. Considering that the preferential orientation of the copper layers is in the direction (111), a possible form in that the small crystals are put in order on the silicon surface following the crystalline direction of this one as is shown in Fig. 6.

On the other hand, for the formation of the tenorite or the cuprite crystalline phase the oxidation temperature is crucial.

The temperature exerts a strong influence on the arrangement of the atoms of the different surfaces of the small crystals. The changes in the ordering of surface atoms determine the type of adsorption centre, in special for oxygen atoms [23].

#### IV. CONCLUSION

Copper oxide layers were obtained successfully with a single crystalline phase cupric o tenorite ( $\text{CuO}$ ,  $\text{Cu}_2\text{O}$ ) on (100) silicon substrates by thermal oxidation using an ambient atmosphere and copper layers. The  $\text{Cu}_2\text{O}$  crystalline phase is obtained with an oxidation temperature of  $200^\circ\text{C}$ , these layers have a refractive index of 2.3. In order to obtain  $\text{CuO}$ , the minimum oxidation temperature was of  $600^\circ\text{C}$ , and its measured refractive index was of 2.75, in both cases, the indices were determined by ellipsometry. Measurements of X-ray diffraction confirmed the presence of the indicated crystalline phases. The grain size calculated by the Debye-Scherrer equation for the predominant direction decreases as the oxidation temperature increases, giving for the Cu nanofilm in the diffraction peak (111), to crystal size of 16.82 nm is obtained. Similarly, for  $\text{Cu}_2\text{O}$ , the nanocrystal size is 8.11 nm and for the  $\text{CuO}$ , the size is 6.66 nm, which indicates that crystal size depends on the annealing.

#### REFERENCES

- [1] Y. Usio, M. Miyayama, H. Yanagida. *Jpn. J. Appl. Phys.* 33 (1994) 1136.
- [2] G. Mangamma, V. Jayaraman, T. Gnanasekaran, G. Peryasamy. *Sensors and Actuators B* 53 (1998) 133.
- [3] W. M. Sears, E. Fortin. *Solar Energy Mater.* 10 (1984) 93.
- [4] A. E. Rakhshani. *Solid State Electron.* 29 (1986) 7.
- [5] N. Ozer, F. Tepehan. *Sol. Energy Mater. Sol. Cells* 30 (1993) 13.
- [6] S. Poulston, P. M. Parlett, P. Stone, M. Bowker. *Surf. Interf. Anal.* 24 (1996) 811.
- [7] J. Li, G. Vizkelethy, P. Revesz, J. W. Mayer. *J Appl. Phys.* 69 (1991) 1020.
- [8] E. M. Alkoy, P. J. Kelly. *Vacuum* 79 (2000) 221.
- [9] X. G. Zheng, M. Suzuki, C. N. Xu. *Mater. Res. Bull.* 33 (1998) 605.
- [10] J. Ghijsen, L. H. Tjeng, J. V. Elp, H. Eskes, J. Westerink, G. A. Sawatzky, M. T. Czyzyk. *Phys. Rev. B* 38 (1988) 11322.
- [11] B. Balamurugan, B. R. Mehta. *Thin Solid Films* 396 (2001) 10.
- [12] T. Tanaka. *Jpn. J. Appl. Phys.* 18 (1979) 1043.
- [13] J. Ramirez-Ortiz, T. Ogura, J. Medina-Valtierra. *Appl. Surf. Sci.* 174 (2001) 177.
- [14] M. Ristov, G. J. Sinadinovski, I. Grozdanov. *Thin Solid Layers* 123 (1985) 63-67.
- [15] J. Lee, Y. Tak. *Electrochemical and Solid-State Letters* 2 (1999) 559.
- [16] R. Kita, K. Kawaguchi, T. Hase, T. Koga, R. Itti, T. Morishita. *J. Mater. Res.* 9 (1994) 1280.
- [17] Y. S. Gong, C. Lee, C. K. Yang. *J. Appl. Phys.* 77 (1995) 5422.
- [18] D. Rönnow, T. Lindström, J. Isidorsson, C. G. Ribbing. *Thin Solid Films* 325 (1998) 92.
- [19] J. J. Burke, N. L. Reed and V. Weiss (Eds.). *Surfaces and Interfaces I. Chemical and Physical Characteristics*. Syracuse University Press. New York (1967) 333.
- [20] T. Sueyoshi, T. Sasaki, Y. Iwasawa. *Surf. Sci.* 365 (1996) 310.
- [21] M. Ottosson, J. Lu, J. O. Carlsson. *J. Crystal Growth* 151 (1995) 305.
- [22] F. Jensen, F. Besenbacher, I. Stensgaard. *Surf. Sci.* 269/270 (1992) 400.
- [23] Y. Xu, M. Mavrikakis. *Surf. Sci.* 494 (2001) 131.
- [24] M. K. Lee, J. J. Wang, H. D. Wang. *J. Electrochem. Soc.* 144 (1997) 1777.
- [25] W. Kern, D. A. Puotinen. *RCA Review* 31 (1970) 187.
- [26] S. R. Kasi, M. Liehr. *J. Vac. Sci. Technol. A: Vacuum Surface and Films* 10 (1992) 795.
- [27] A. F. Trotman-Dickenson (Ed.). *Comprehensive Inorganic Chemistry*, vol. 3, Pergamon, Oxford. (1973) 16.
- [28] M. T. S. Nair, L. Guerrero, O.L. Arenas, P.K. Nair. *Appl. Surf. Sci.* 150 (1999) 143.
- [29] J. Wang, V. Sallet, F. Jomard, A. Rego, E. Elangovan, R. Martins, E. Fortunato, *Thin Solid Films* 515 (2007) 8780.
- [30] S. P. Murarka, S. W. Hymes. *Crit. Rev. Solid State Mater. Sci.* 20 (1995) 87.